Nuclear Magnetic Resonance Imaging of Liver Hemangiomas

R. Sigal, A. Lanir, H. Atlan, J. E. Naschitz, J. S. Simon, R. Enat, D. Front, O. Israel, R. Chisin, Y. Krausz, Y. Zur, and N. Kaplan

Department of Medical Biophysics, Hadassah University Hospital, Jerusalem; Department of Biochemistry, Haifa Medical Center (Rothschild); Department of Nuclear Medicine, Rambam Medical Center, Haifa; and Elscint MRI Center, Herzlia, Israel

Nine patients with cavernous hemangioma of the liver were examined by nuclear magnetic resonance imaging (MRI) with a 0.5T superconductive magnet. Spin-echo technique was used with varying time to echo (TE) and repetition times (TR). Results were compared with ^{99m}Tc red blood cell (RBC) scintigraphy, computed tomography (CT), echography, and arteriography. Four illustrated cases are reported. It was possible to establish a pattern for MRI characteristics of cavernous hemangiomas; rounded or smooth lobulated shape, marked increase in T_1 and T_2 values as compared with normal liver values. It is concluded that, although more experience is necessary to compare the specificity with that of ultrasound and CT, MRI proved to be very sensitive for the diagnosis of liver hemangioma, especially in the case of small ones which may be missed by ^{99m}Tc-labeled RBC scintigraphy.

J Nucl Med 26:1117–1122, 1985

Many reports have documented the ability of magnetic resonance imaging (MRI) to display normal and abnormal anatomy of the liver (*1–8*). However, few cases of cavernous hemangiomas have been described in the literature (*1,3,7*) although it is the most common benign liver tumor (*9*). They are generally asymptomatic and are noted incidentally in postmortem investigations; however, in some cases, their existence is suspected either because they become manifest clinically or as a result of an incidental finding during an abdominal imaging procedure [technetium-99m (^{99m}Tc) sulfur colloid scintigraphy, ultrasound or computed tomography (CT)] performed for an unrelated problem. In such cases, differentiation with other space-occupying lesions, hepatomas and metastases in particular, is mandatory; because of a high bleeding risk after percutaneous biopsy, the diagnosis must be established or ruled out before such a procedure is decided. To this respect, radionuclide liver scans using ^{99m}Tc-labeled red blood cells ([^{99m}Tc]RBCs) allow for characterization of this kind of liver lesion when delayed blood-pool imaging is performed (*10–12*). However, it may fail to detect small masses, particularly in cases of extensive fibrosis within the tumor. In such cases, radionuclide angiogram with flow study has been recently recommended (*12*); however, its contribution remains to be precisely determined. Likewise, the role of CT, with pre- and postcontrast scans, is still controversial (*13–14*). For these reasons, angiography is performed when the result of the RBC scintigraphy is still doubtful. This study analyzes the MRI characteristics of liver cavernous hemangiomas and compares the MRI findings with [^{99m}Tc]RBC scintigraphy, ultrasound, CT, and angiography.

Received Jan. 25, 1985; revision accepted June 20, 1985.

For reprints contact: H. Atlan, MD, PhD, Dept. of Medical Biophysics, Hadassah University Hospital, Jerusalem, Israel.

MATERIALS AND METHODS

NMR imaging techniques

MRI was performed with a superconducting magnet* operating a 0.5T (21.3 MHz). In all cases, an elliptical body coil with a 57 × 37 cm aperture and a 60 cm length was employed. Spatial resolution was 1.2 mm horizontal and 2.3 mm vertical. All images were obtained using a two-dimensional Fourier transform technique. Data were collected on a 256 × 128 matrix interpolated to 256 × 256 density reconstruction. Sliced thickness varied from 5 to 10 mm and sequential imaging planes were 2 or 3 mm apart. Imaging was obtained in direct axial, coronal, and sagittal planes. Multi-echo, multislice imaging was used, the total

TABLE 1
Imaging Procedures Which Visualized Liver Hemangiomas in Nine Patients

Patient no./age/sex	Ultrasonography	[^{99m}Tc]colloid and dynamic [^{99m}Tc]RBC scan	CT	Arteriography	Laparotomy	MRI
1 53 yr (F)	X	X	X	X	—	X
2 53 yr (F)	X	X	—	X	—	X
3 65 yr (M)	X	X	X	X	—	X
4 41 yr (F)	X	X	—	—	—	X
5 63 yr (M)	X	X	—	X	—	X
6 40 yr (F)	X	X	—	—	X	X
7 26 yr (M)	X	X	—	X	X	X
8 43 yr (F)	X	X	—	—	—	X
9 34 yr (F)	X	X	—	—	—	X

number of slices per scan depending upon the acquisition protocol. All images were obtained from spin-echoes with echo delay time (TE) of 29 and 58 msec (first and second-echo, respectively). The repetition time per cycle (TR) varied from 179 msec to 2,500 msec; in most cases averaging two signals was sufficient to get a good signal to noise ratio. Thus, the scanning time varied from 45 sec to 21.2 min depending upon the TR. Every patient was imaged using at least two different TR, so as to obtain T_1 weighted images (short TR) and T_2 weighted images (long TR). Thus, T_1 and T_2 relaxation times could be estimated from the intensity data, using the method of Herfkens et al. (15). This method uses the ratio of intensities produced by different TR to calculate T_1 and different TE to calculate T_2. Intensity measurements of different tissues within the same image or from one image to another can be compared if standardization is performed using external (phantom) or internal reference standard (paraspinous muscles in this study).

Patient population and case history

Twenty patients underwent MRI examination of the upper abdomen. Informed consent was obtained in all cases. Among them, six patients, aged 15–76 yr, without liver disease were being evaluated for pancreatic, renal, or splenic abnormalities. Five volunteers served as control subjects. Thus, 11 patients were used as controls with normal liver documented by normal ultrasonographies and [^{99m}Tc]colloid liver-spleen scintigraphies. In addition, nine patients aged 26–65 yr, with diagnosed liver hemangiomas, underwent liver nuclear magnetic resonance (NMR) imaging. The diagnosis was based on the combination of other imaging procedures, namely ultrasonography, radionuclide scintigraphies including [^{99m}Tc]tin colloid scan, and [^{99m}Tc]RBC dynamic scintigraphies with early and 1-hr delayed scans, and x-ray CT with precontrast and postcontrast scans. A selective arteriography with injection into the hepatic artery was performed in four cases and a laparotomy in two cases. Needle biopsy puncture was not performed due to a high abdominal bleeding risk. In three cases, the findings on [^{99m}Tc]RBC scintigraphies were considered specific enough (*10–12*) to make the diagnosis with no need for additional invasive procedures (Table 1).

RESULTS

The normal liver was demonstrated on spin-echo images as a homogeneous organ of moderate intensity. Hepatic veins, portal veins, and hepatic arteries were visualized as low intensity structures. Using different imaging planes, hepatic size and volume could be calculated. The signal intensity of hepatic hemangiomas, compared with normal liver, was dependent upon the NMR imaging parameters used to get the image. Using short TR (179 msec) and TE (29 msec), hemangiomas appeared with a lower intensity than the liver; with the lengthening of TR (up to 2,500 msec) and TE (58 msec) hemangiomas were visualized as high-intensity masses relative to the rest of the liver (Fig. 9). In general, the best contrast between hemangiomas and liver was obtained using a long interval between pulse sequences (TR = 1,500 msec or 2,500 msec) and a long time to echo (58 msec). Some hemangiomas were almost indistinguishable from the surrounding hepatic tissue when imaged with short TR and TE sequences. The trend towards very high signal intensities, when imaged with long TR and TE sequences, was established in all cases. Likewise, all tumors presented a more or less inhomogeneous aspect probably depending on the amount of sclerosis. The contours of the lesions were grossly irregular in most cases with a smooth lobulated appearance. However, although the margin of the tumor appeared generally slightly regular, none presented a round, even contour.

MRI was of particular interest in demonstrating the tumor size and location and its relationship with intra and extrahepatic structures, particularly hepatic vasculature. Both lobes of the liver were involved in five cases and only the right in four cases. The dimension of the largest tumor was 27 cm long, 16 cm high, 13 cm deep (Fig. 2A,B). Small-size hemangiomas were readily

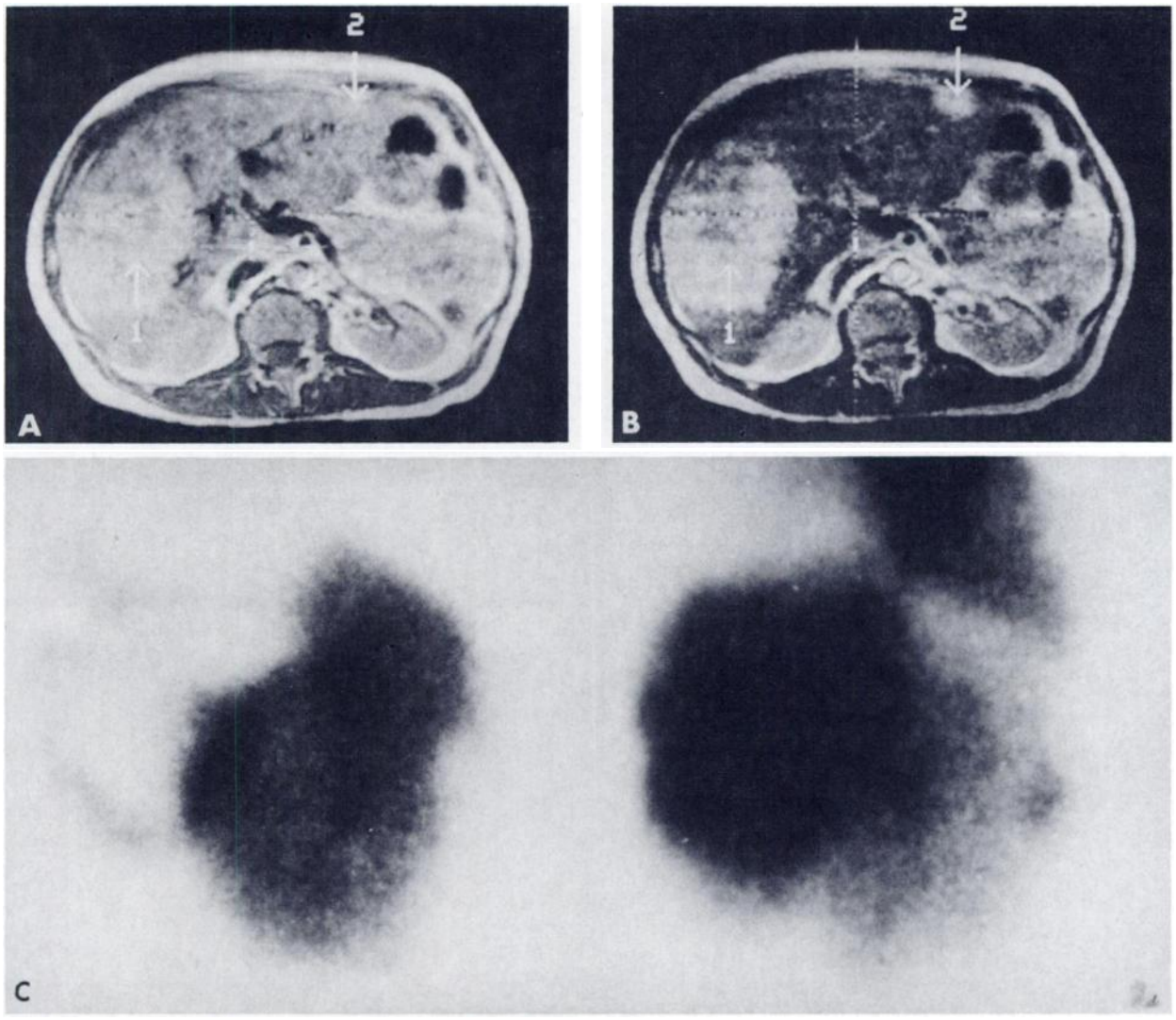

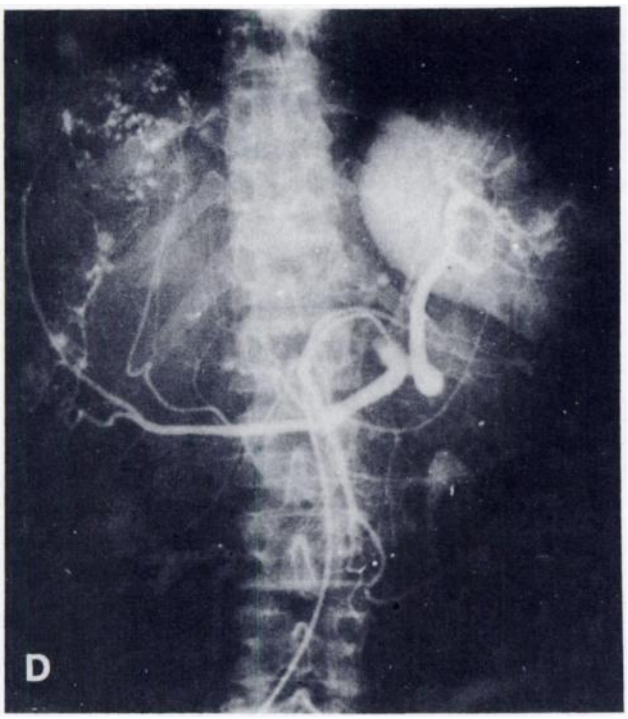

FIGURE 1
Hemangioma of liver. MRI axial scans. A: 1,500 msec TR, 29 msec TE: Larger hemangioma in right lobe (arrow 1) and small one located in left lobe (arrow 2) are hardly distinguishable from surrounding parenchyma. B: 1,500 msec TR, 58 msec TE: With increasing of TE, both hemangiomas are readily checked as high intensity structures. Note areas of unhomogeneity within larger one. C: [^{99m}Tc]tin colloid liver scintigraphy (left) showing large SOL in right lobe and small imprint in border of left. [^{99m}Tc]RBC angioscintigraphy (right) showing filling of these two defects corresponding to big and small hemangioma respectively, as seen in MRI images. However, small one is doubtful and can be missed without previous knowledge of MRI finding. This is indication that MRI may be more sensitive than usual radioisotope scanning for small lesions. D: Selective hepatic arteriography showing large vascular area corresponding to MRI finding

checked (Figs. 1C,3B) as well as areas containing minute, confluent lesions which could not be measured adequately (Table 2).

T_1 and T_2 values of the liver of control patients were calculated and the average value was respectively T_1 =

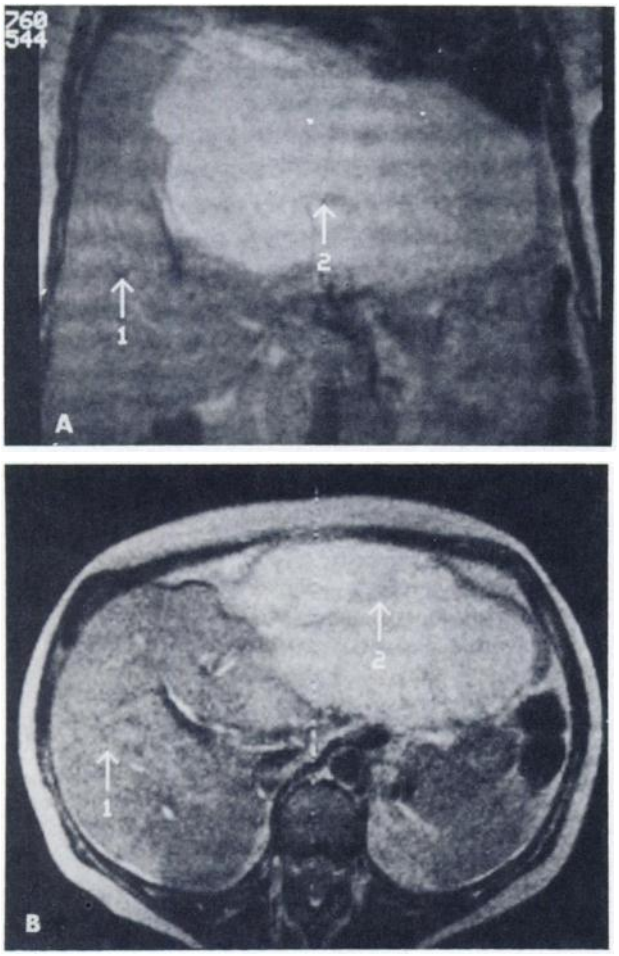

FIGURE 2
Giant hemangioma of liver. A: Coronal scan 1,500 msec TR, 58 msec TE. B: Axial scan 1,500 msec TR, 58 msec TE. Relationship between tumor (arrow 2) and rest of liver (arrow 1) is clearly depicted by combination of two imaging planes

375 msec (range 340–430, s.d. = 32 msec), and T_2 = 42 msec (range 36–48, s.d. = 4 msec). The T_1 and T_2 values of the hemangiomas in four patients could be calculated and were significantly longer than in normal liver with average values, respectively, T_1 = 1,100 ± 110 and T_2 = 108 ± 19 msec (see Table 2).

Four of the patients underwent angiography, with selective hepatic artery catheterization. A gross overlapping with the data obtained by MRI was observed. In particular the numerous unifocal or conglomerate vascular lakes which are seen early in the arterial phase and persist into the venous phase corresponded topographically to the lesions depicted by MRI. However, although angiography remains the reference diagnostic procedure, it has the disadvantage of being invasive.

The patient history of four illustrated cases will be presented. It exemplifies the different attitudes adopted today in different institutions to handle these patients, as it is apparent also in the current literature (*10–14*).

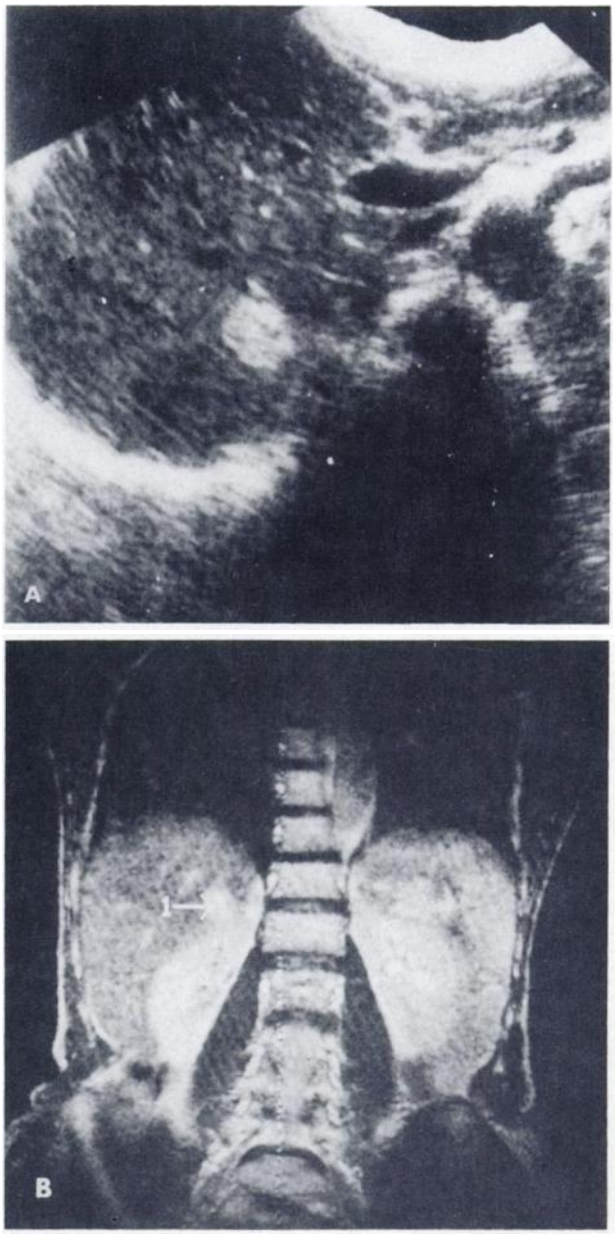

FIGURE 3
A: Transverse sonogram of left lobe of liver. Small echogenic mass sharply defined from normal liver. B: Spin-echo MRI coronal scan 1,500 msec TR, 58 msec TE demonstrates area with increased signal intensity (arrow 1); in addition many minute confluent lesions can be seen

CASE REPORTS

Case 1

A 44-yr-old female was referred to our outpatient surgical clinic because vague abdominal pains and discomfort had increased in intensity the prior few months. No abnormal findings were noted on physical examination or on hepatic function tests. An ultrasonography of the abdomen revealed a large space occupying lesion (SOL) in the right lobe of the liver, confirmed by liver-spleen [^{99m}Tc]colloid scan and x-ray CT. This SOL filled up on [^{99m}Tc]RBC dynamic and static scin-

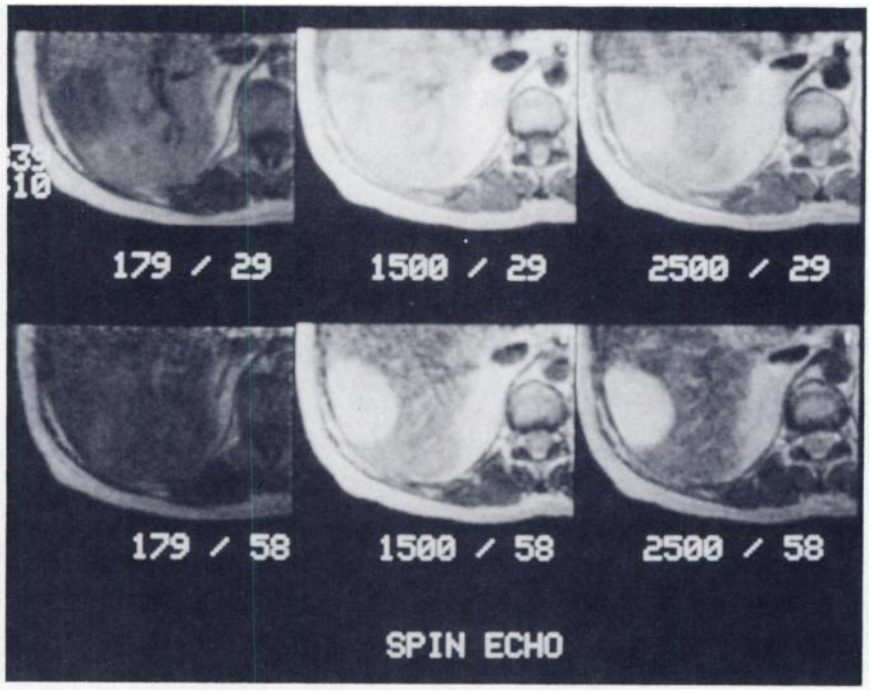

FIGURE 4
Middle-sized hemangioma in right lobe of the liver. Effect of lengthening TR and TE. Axial spin-echo NMR scans zoomed on right posterior quadrant. TR and TE are indicated as, respectively, first and second numbers. On T_1 weighted images (upper left) hemangioma is seen with less signal than surrounding normal liver indicating long T_1. Signal intensity of hemangioma increases with lengthening of TR and TE

tigraphies, more on delayed scans (Fig. 1C). An arteriography was performed and showed a typical pattern of hemangioma in the right lobe (Fig. 1D). The NMR imaging confirmed the findings in the right lobe but revealed an additional small SOL with the same intensity parameters in the left lobe (Fig. 1A,B). In retrospect this small hemangioma can also be recognized on the [^{99m}Tc]RBC scintigraphies (Fig. 1C).

Case 2

A 53-yr-old female consulted the outpatient clinic because of transient diarrhea without any other symptoms. On physical examination hepatomegaly was noted, reaching 5–8 cm below the costal margin. The results of an ultrasonography, [^{99m}Tc]colloid scan, and angiographic procedures were consistent with a large hepatic tumor. Typical patterns of a giant cavernous hemangioma of the left lobe of the liver were obtained by [^{99m}Tc]RBC scintigraphies and selective arteriography. The NMR imaging of the abdomen showed a giant mass of the left lobe extending to the right lobe, the limits of which were clearly outlined by the combination of two imaging planes (Fig. 2A,B).

Case 3

A 65-yr-old male was referred to our outpatient clinic because of attacks of diffuse abdominal pains. There were no pathological findings as a result of clinical examination and laboratory tests. Nondocumented surgery for a tumor of the spine occurred 7 yr previously. An ultrasonography disclosed a small SOL of the liver (Fig. 3A) confirmed by CT. Technetium-99m colloid and [^{99m}Tc]RBC scans gave doubtful results. A selec-

TABLE 2
Characteristics of Lesions as Depicted by MRI

Patient no.	No. of lesions	Site			Dimension		Irregular contour and non-homogeneous aspect			Minute confluent lesions	T_1 msec	T_2 msec
		Right lobe	Left lobe	Both	Largest dimension of lesions (cm)	Smallest dimension of lesions (cm)	Large lesions	Medium lesions	Small lesions			
1	2	—		X	18	5	X	—	—	—	—	—
2	1	—		X	27	13	X	—	—	—	1,080	105
3	1	X		—	2	—	—	—	—	X	—	—
4	1	X		—	6	—	—	—	—	—	1,120	114
5	1	X		—	13	—	—	—	—	—	1,170	120
6	2	—		X	15	4	X	X	—	X	—	—
7	4	—		X	5	0.5	X	X	—	X	—	—
8	4	—		X	10	1	X	X	X	—	—	—
9	1	X		—	20	—	X	—	—	—	1,020	95

tive arteriography was performed and showed a typical pattern of liver hemangioma in the right lobe. The NMR image of the liver showed a small irregular area of increased signal intensity in the right lobe with minute confluent lesions, better visualized on T_2 weighted images (Fig. 3B).

Case 4

A 41-yr-old female was hospitalized for workup after the discovery of different echogenic regions in the liver by ultrasonography in an out-patient clinic. There were complaints of abdominal pain in the right upper quadrant for 13 yr, especially after meals, more frequent and intense in the prior few months. There were no pathological findings on clinical examination except for tenderness in the epigastrium. Laboratory tests and x-rays of upper and lower GI were normal. A [^{99m}Tc]colloid liver-spleen scan revealed a focal lesion in the postero-lateral region of the right lobe of the liver. Dynamic [^{99m}Tc]RBC scintigraphies showed a delayed filling of the lesion, typical of liver hemangiomas. The patient was discharged without treatment and accepted to be examined by MRI. The NMR imaging of the liver showed a distinct mass in the postero-lateral part of the right lobe with no additional lesion. Use of several repetition times allowed observation of pulse sequences where the combined effects of T_1 and T_2 increases would compensate one another and the mass could be missed, and of optimum pulse sequences giving the best tumor to normal tissue contrast (Fig. 4).

DISCUSSION

In our overall study of nine patients with 17 lesions the sensitivity of NMR imaging appeared very high (100%) since none of the hemangiomas documented by any other method was missed. The question therefore arises as to whether MRI, which does not appear to have any biological risks, could be specific enough to avoid the need of angiography. It was possible to establish a pattern for MRI characteristics of cavernous hemangiomas; rounded or smooth lobulated shape, absence of peripheral rim and septations and, moreover, a general trend towards high T_1 and T_2 values as compared to normal liver values. The significance of this increase to T_1 and T_2 is difficult to assess since an unknown flow factor is likely to modify the signal intensity in a nonhomogeneous way, in various areas of the tumor. An augmentation of the relaxation times is also described in the literature when dealing with other liver tumors, primary or metastatic (*1,5*); however, in such cases, there are many exceptions in which the relaxation time values, T_2 in particular, are shorter than those of normal liver parenchyma (*3,5*).

Moreover, in this study there was no overlap between normal and pathological values; the average increase in relaxation time was 83% for T_1 and 50% for T_2, and in both cases these variations were observed on a relatively narrow range.

Therefore, in order to assess the specificity of NMR imaging for the diagnosis of liver hemangioma, we must learn to discriminate this pattern from other tumors of the liver. However, the association of [^{99m}Tc]RBC dynamic scintigraphies (high specificity) and NMR imaging (high sensitivity) seems to be the combination of choice, and it can be foreseen that MRI will play a prominent role in establishing the diagnosis of liver hemangioma particularly when some doubts remain after RBC radionuclide scintigraphy.

FOOTNOTE

* Elscint Gyrex S-5000.

REFERENCES

1. Smith FW, Mallard JR, Reid A, et al: NMR tomographic imaging in liver disease. *Lancet* 1:963-966, 1981
2. Doyle FH, Pennock JM, Banks LM, et al: NMR imaging of the liver: Initial experience. *Am J Roentgenol* 138:193-200, 1982
3. Buonocore E, Borkowski GP, Pavilicek W, et al: NMR imaging of the abdomen, technical considerations. *Am J Roentgenol* 141:1171-1178, 1983
4. Borkowski GP, Buonocore E, George CR, et al: NMR imaging in the evaluation of the liver: A preliminary experience. *JCAT* 7(5):768-774, 1983
5. Margulis AR, Moss AA, Crooks LE, et al: NMR in diagnosis of tumors of the liver. *Semin Roentgenol* XVIII(2):123-126, 1983
6. Stark DD, Goldbert HI, Moss AA, et al: Chronic liver disease: Evaluation by magnetic resonance. *Radiology* 150:149-151, 1984
7. Moss AA, Goldbert HI, Stark DB, et al: Hepatic tumors: Magnetic resonance and CT appearance. *Radiology* 150:141-147, 1984
8. Wenker JC, Baker MK, Ellis JH, et al: Focal fatty infiltration of the liver: Demonstration by MRI. *Am J Roentgenol* 143:573-574, 1984
9. Ishak KG, Rabin L: Benign tumors of the liver. *Med Clin North Am* 59:995-1013, 1975
10. Front D, Royal HD, Israel O, et al: Scintigraphy of hepatic hemangiomas: The value of Tc-99m labeled red blood cells: Concise communication. *J Nucl Med* 22:684-687, 1981
11. Engel MA, Marks PS, Sandler MA, et al: Differentiation of focal intrahepatic lesions with 99m Tc red blood cell imaging. *Radiology* 146:777-782, 1983
12. Rabinowitz SA, McKusick DA, Strauss HW: 99mTc red blood cell scintigraphy in evaluating focal liver lesions. *Am J Roentgenol* 143:63-68, 1984
13. Barnett PH, Zerhouni EA, White RI, et al: Computed tomography in the diagnosis of cavernous hemangioma of the liver. *Am J Roentgenol* 134:439-447, 1982
14. Burgener FA, Hemlin DJ: Contrast enhancement of focal hepatic lesions in CT: Effect of size and histology. *Am J Roentgenol* 140:297-301, 1983
15. Herfkens R, Davis P, Crooks LE, et al: MNR imaging of the abnormal live rat and correlations with tissue characteristics. *Radiology* 141:211-218, 1981